



ChemComm

**The effect of amorphization on the molecular motion of the  
2-methylimidazolate linkers in ZIF-8**

Journal:	<i>ChemComm</i>
Manuscript ID	CC-COM-04-2019-002673.R1
Article Type:	Communication

SCHOLARONE™  
Manuscripts

## COMMUNICATION

Received 00th January  
20xx,

## The effect of amorphization on the molecular motion of the 2-methylimidazolate linkers in ZIF-8

Naoki Ogiwara,<sup>a</sup> Daniil I. Kolokolov,<sup>\*b,c</sup> Masaki Donoshita,<sup>a</sup> Hirokazu Kobayashi,<sup>a,d</sup> Satoshi Horike,<sup>e</sup>  
Alexander G. Stepanov,<sup>b,c</sup> and Hiroshi Kitagawa<sup>\*a,e</sup>

Accepted 00th January 20xx

DOI: 10.1039/x0xx00000x

**We investigated the effect of amorphization on the mobility of the 2-methylimidazolate linkers in ZIF-8. Solid-state <sup>2</sup>H NMR studies revealed that amorphization significantly affects the mobility of the linkers, including the rotational angle and speed. Furthermore, a new intermediate librational mode appeared in amorphous ZIF-8.**

Molecular motion in solids is an important phenomenon because it strongly correlates to a wide range of physicochemical properties, such as dielectric,<sup>1</sup> magnetic,<sup>2</sup> and optical properties.<sup>3</sup> Hence, a rational design to control molecular dynamics is a critical strategy for the development of functional materials.<sup>4</sup> Metal–organic frameworks (MOFs), constructed from metal ions and organic linkers, have attracted increasing attention as a promising platform to design materials with controllable structural mobility due to their structural diversity derived from numerous available choices of constituents.<sup>5–8</sup> The remarkably high designability/tunability of MOFs is very useful to effectively control the molecular motion and associated functions, such as gas diffusion,<sup>9,10</sup> luminescence,<sup>11</sup> and spin crossover.<sup>12</sup>

Amorphous MOFs ( $a_m$ MOFs), lacking any long-range order but retaining the basic metal–linker connectivity of the crystalline MOFs, have emerged as a new class of materials in the maturing field of MOFs in recent years.<sup>13</sup> Due to their highly disordered structures,  $a_m$ MOFs contribute to improving the functionalities of ionic<sup>14</sup> or electronic<sup>15</sup> conductivity of the

crystalline phase. Furthermore,  $a_m$ MOFs have intrinsic mechanical properties<sup>16</sup> and inherent porosity,<sup>17</sup> offering the irreversible trapping of guest molecules<sup>18</sup> and prolonged controlled release of therapeutic agents,<sup>19</sup> which are not achievable with the mother MOF crystals. Thus, since some advantages of  $a_m$ MOFs are attributable to the modulation of the guest diffusion, a clarification of the dynamic motion, such as the flip-flop motion of ligands (restricted rotations of the linker's plane by 2-site jumps between two stable orientations), is important for obtaining a better understanding of the diffusion in  $a_m$ MOFs. However, not many studies have yet been carried out on the dynamic motion of  $a_m$ MOFs, whereas much effort has been devoted to disclosing the static amorphous structure.<sup>13,16,20</sup> Here, we investigated, for the first time, the influence of amorphization on the motion exhibited by linkers in MOFs.

We selected ZIF-8 [ $\text{Zn}(2\text{-mIM})_2$ ] (2-mIM = 2-methylimidazolate) for use in this study.<sup>21,22</sup> ZIF-8 is one of the most well known MOFs; it has been widely studied not only for its fundamental properties (mechanical properties,<sup>23</sup> molecular motion,<sup>24–26</sup> etc.) but also for its practical applications, such as separation,<sup>27</sup> heterogeneous catalysts,<sup>28</sup> and sensors.<sup>29</sup> Synthetic procedures for amorphous ZIF-8 prepared by ball-milling ( $a_m$ ZIF-8) also have been developed.<sup>30,31</sup>

To address the mobility of ligands in  $a_m$ ZIF-8, we made use of <sup>2</sup>H solid-state NMR spectroscopy, which is a well established technique to probe the mobility of molecules in solid materials. <sup>2</sup>H NMR line shape, being defined completely by intramolecular quadrupole interaction, is quite sensitive to the type and the rate of the molecular motion. Spin–lattice and spin–spin relaxation times ( $T_1$  and  $T_2$ ) also provide valuable information on the energetics and the rate of the different intramolecular and intermolecular motions.<sup>32,33</sup>

In a typical synthesis, deuterated ZIF-8 crystals were prepared in MeOH solution (pH mediated) at room temperature.<sup>25</sup> The amorphization of ZIF-8 was performed using the ball milling method to obtain deuterated  $a_m$ ZIF-8.<sup>20</sup>

<sup>a</sup> Division of Chemistry, Graduate School of Science, Kyoto University, Kitashirakawa-Oiwakecho, Sakyo-ku, Kyoto, 606-8502, Japan.  
E-mail: kitagawa@kuchem.kyoto-u.ac.jp

<sup>b</sup> Borekov Institute of Catalysis, Siberian Branch of Russian Academy of Sciences, Prospekt Akademika Lavrentieva 5, Novosibirsk 630090, Russia  
E-mail: mailto:kdi@catalysis.ru

<sup>c</sup> Novosibirsk State University, Pirogova Street 1, Novosibirsk 630090, Russia

<sup>d</sup> PRESTO, Japan Science and Technology Agency, 4-1-8 Honcho, Kawaguchi, Saitama 332-0012, Japan

<sup>e</sup> Institute for Integrated Cell-Material Sciences, Institute for Advanced Study, Kyoto University, Yoshida-Honmachi, Sakyo-ku, Kyoto 606-8501, Japan

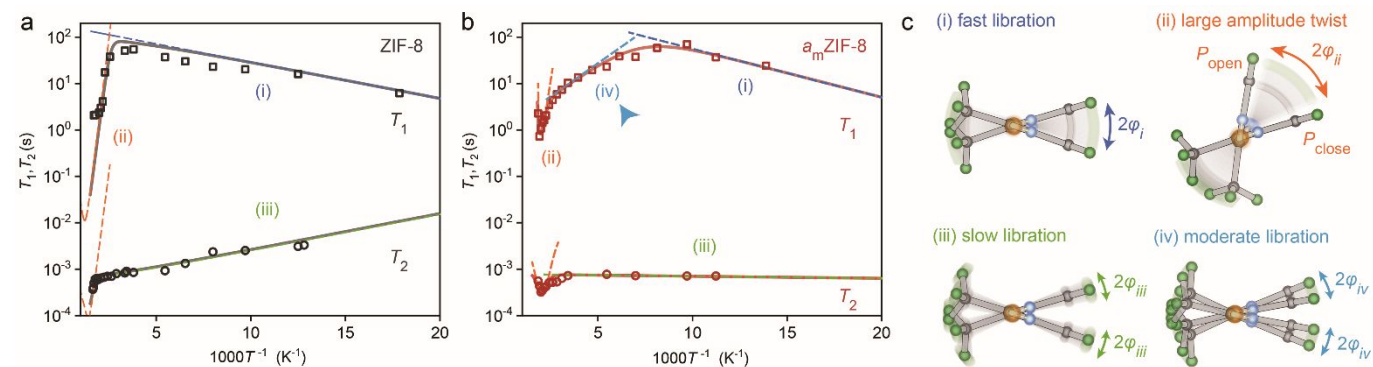
Electronic Supplementary Information (ESI) available: [details of any supplementary information available should be included here]. See DOI: 10.1039/x0xx00000x

The powder X-ray diffraction patterns of  $a_m$ ZIF-8 showed broad peaks due to the lack of long range structural periodicity (Fig. S1). The Zn-K edge X-ray absorption spectra (XAS) revealed that the local structure of  $a_m$ ZIF-8 was identical to that of ZIF-8 crystals (Figs. S2–S4), indicating that  $a_m$ ZIF-8 retains the coordination geometry around the Zn<sup>2+</sup> ions of the crystalline phase. The N<sub>2</sub> sorption isotherm at 77 K and the calculated BET surface area confirmed that  $a_m$ ZIF-8 has nonporous character originating from an amorphous structure (Fig. S5), which is in agreement with previously reported results.<sup>20</sup>

To investigate the mobility of 2-mIM in  $a_m$ ZIF-8, we first recorded <sup>2</sup>H solid-state NMR spectra. Fig. 1 shows that the <sup>2</sup>H NMR spectra of  $a_m$ ZIF-8 exhibit two signals, corresponding to the rapidly rotating CD<sub>3</sub> groups of 2-mIM (narrow axially symmetric pattern) and the CD groups (broad axially symmetric pattern) of 2-mIM as in the case of ZIF-8 crystals.<sup>25</sup> These results imply that the type of motion of the linkers remains unchanged between ZIF-8 crystals and  $a_m$ ZIF-8.

It was evident, however, that the <sup>2</sup>H NMR line shape analysis could not address changes in the framework dynamics by amorphization. Therefore, we subsequently performed variable temperature  $T_1$  and  $T_2$  measurements in an effort to understand the difference in molecular motion. First, we considered the mobility of the 2-mIM CD groups because their dynamics directly map the mobility of the whole linker (Fig. 2 and Fig. S6). In ZIF-8 crystals, the CD groups followed three types of motion:<sup>26</sup> (i) fast restricted libration; (ii) slower, large amplitude twist of the linker (“the gate opening motion”); and (iii) a slow restricted libration, associated with the “soft vibrational modes” of the whole framework. On the other hand,  $a_m$ ZIF-8 gave not

**Fig. 2.** <sup>2</sup>H NMR  $T_1$  (squares) and  $T_2$  (circles) relaxation curves as a function of temperature for the CD group of the 2-mIM linker in



only these three modes observed in the crystalline phase but also a new mode of motion, (iv). This mode is rationalized as an additional restricted libration with the intermediate rate. To quantitatively compare ZIF-8 with  $a_m$ ZIF-8 for individual motional modes, we proceeded to further analyze the experimentally obtained  $T_1$  and  $T_2$  curves by a numerical fitting using the general formalism based on the Bloch–Wangsness–Redfield NMR relaxation theory<sup>34</sup> extended for the presence of additional slow anisotropic motions<sup>33</sup> (see ESI for details). The resulting rotational angles ( $\varphi$ ), the activation barriers ( $E_a$ ), and rate constants ( $\tau$ ) for each mode are given in Table 1.

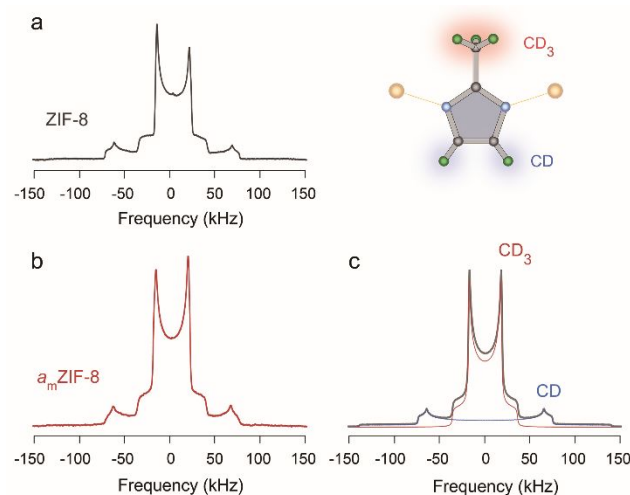


**Fig. 1.** <sup>2</sup>H NMR line shape for 2-mIM of (a) ZIF-8 and (b)  $a_m$ ZIF-8 at 295 K. (c) The numerical simulation. Summation is shown in gray, the CD<sub>3</sub> groups in red, and the CD groups in blue.

(a) ZIF-8 and (b)  $a_m$ ZIF-8. The numerical simulation results are given by solid lines. Dashed lines emphasize individual motional modes. (c) Schematic illustration of the four main motions in the presence of  $a_m$ ZIF-8.

**Table 1.** Fitting parameters for  $T_1$  and  $T_2$  relaxation in ZIF-8 and  $a_m$ ZIF-8.

	mode (i)			mode (ii)			mode (iii)			mode (iv)			mode (v)		
	$\varphi_i$ (°)	$E_{a,i}$ (kJ mol <sup>-1</sup> )	$\tau_i$ (s)	$\varphi_{ii}$ (°)	$E_{a,ii}$ (kJ mol <sup>-1</sup> )	$\tau_{ii}$ (s)	$\varphi_{iii}$ (°)	$E_{a,iii}$ (kJ mol <sup>-1</sup> )	$\tau_{iii}$ (s)	$\varphi_{iv}$ (°)	$E_{a,iv}$ (kJ mol <sup>-1</sup> )	$\tau_{iv}$ (s)	$\varphi_v$ (°)	$E_{a,v}$ (kJ mol <sup>-1</sup> )	$\tau_v$ (s)
ZIF-8	± 17	1.5	$8.9 \times 10^{-14}$	80°	60	$2.3 \times 10^{12}$	± 6	1.5	$1.3 \times 10^{-6}$	--	--	--	70.5	1.5	$5.3 \times 10^{-13}$
$a_m$ ZIF-8	± 17	2	$2.3 \times 10^{-14}$	48°	50	$3.2 \times 10^{13}$	± 6	0.1	$1.9 \times 10^{-7}$	± 6	5.5	$4.0 \times 10^{-9}$	70.5	3.8	$7.3 \times 10^{-13}$

$Q_{CD}$  = 203 kHz for modes (i)–(iv) and  $Q_{CD_3}$  = 170 kHz for mode (v).  $\tau = 1/(k 2\pi)$ , where  $k$  is given in Hz. The error for activation energy barriers is 10%. It is 20% for the pre-exponential factors and 10% for the angles. The equilibrium population of the open state ( $P_{open}$ ) for the mode (ii) of ZIF-8 and  $a_m$ ZIF-8 was 0.1 and 0.01, respectively. The  $P_{eq}$  for the other motions were equivalent for all the sites.

## COMMUNICATION

The  $\varphi_{ij}$ ,  $E_{a,ij}$ , and  $\tau_i$  of the fast restricted librational motion (i) for  $a_m$ ZIF-8 were estimated to be  $\pm 17^\circ$ ,  $2.0 \text{ kJmol}^{-1}$ , and  $2.3 \times 10^{-14} \text{ s}$ , respectively, which are almost same as for the crystalline phase. Observations indicated that changes in the torsional potential of the linkers induced by amorphization did not significantly affect the small angular displacement. In contrast, the large amplitude twist mode (ii) underwent a notable change upon amorphization. The rate constants of  $a_m$ ZIF-8 became faster ( $\tau_{ii}(a_m\text{ZIF-8}) \sim 5.3 \times 10^{-8} \text{ s} < \tau_{ii}(\text{ZIF-8}) \sim 4.2 \times 10^{-6} \text{ s}$ , at 500 K) but the rotational angles were much more restricted in terms of amplitude ( $\varphi_{ii}(a_m\text{ZIF-8}) \sim 48^\circ < \varphi_{ii}(\text{ZIF-8}) \sim 80^\circ$ ). The large amplitude twist was further characterized by the equilibrium population of the open state ( $P_{\text{open}}$ ). The  $P_{\text{open}}$  in  $a_m$ ZIF-8 decreased to 0.01, which is 10 times smaller than that of ZIF-8 ( $P_{\text{open}} = 0.1$ ). This clarifies larger hindrances for large amplitude rotation in the amorphous phase. The observation is in line with the disappearance of hysteresis in the  $\text{N}_2$  sorption isotherm (Fig. S5). The libration amplitude of the slow librational mode (iii) for  $a_m$ ZIF-8 ( $\varphi_{iii} = \pm 6^\circ$ ) is consistent with that for ZIF-8 ( $\varphi_{iii} = \pm 6^\circ$ ), whereas mode (iii) in  $a_m$ ZIF-8 becomes almost barrierless ( $E_{a,iii} = 0.1 \text{ kJmol}^{-1}$ ) and the rate constant *ca.* 10 times faster ( $\tau_{iii} = 1.9 \times 10^{-7} \text{ s}$ ). This is probably because the amorphous phase has a highly disordered structure and could effectively transport the phonon vibrations. The new librational mode (iv) in  $a_m$ ZIF-8 is rather peculiar as it is an activation process, with a barrier only slightly larger than for the fast librations (i) but an intermediate motional rate. However, simultaneously, it is very restricted in the angular amplitude, as in the case of the slow mode (iii) ( $\varphi_{iv} = 12^\circ$ ). Its presence may indicate that the amorphous phase has an additional collective vibration mode of the lattices and/or an additional degree of freedom in the torsional potential responsible for local rotations of the linkers compared with the crystalline phase.

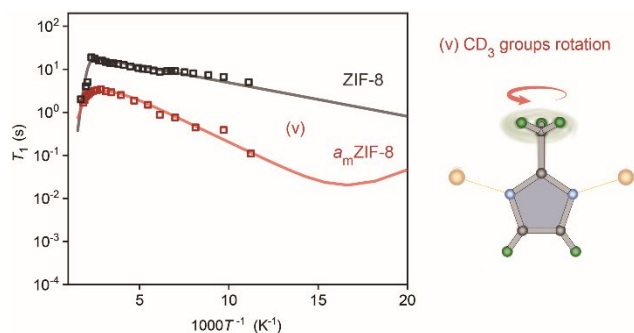


**Fig. 3.**  $^2\text{H}$  NMR  $T_1$  relaxation curves as a function of temperature for the  $\text{CD}_3$  groups of the deuterated 2-mIM linker in ZIF-8 (black) and  $a_m$ ZIF-8 (red). The numerical simulation results are given by solid lines.

We also investigated the dynamics of the  $\text{CD}_3$  groups in 2-mIM by  $T_1$  relaxation measurement (Fig. 3). Curves for both the crystalline and amorphous phases could be simulated within the same model, as for the CD groups, with an addition of the axially symmetric  $\text{CD}_3$  groups' rotation (mode (v), Table. 1, Fig. S7). In ZIF-8 crystals, the  $\text{CD}_3$  groups rotate in the absence of almost any restrictions due to their specific orientation in the void of the ZIF-8 cavity. On the other hand, in the amorphous phase, the  $\text{CD}_3$  groups' rotation mode (v) is characterized by much slower rotation rates ( $\tau_v \sim 7.3 \times 10^{-13} \text{ s}$ ) due to a much higher activation barrier (more than twice as high) ( $E_{a,v} \sim 3.8 \text{ kJmol}^{-1}$ ). The regulated  $\text{CD}_3$  groups' rotation is attributable to the loss of nanoporous nature in  $a_m$ ZIF-8 (Fig. S5).

In summary, we have studied, for the first time, the effect of amorphization on the dynamics of the linkers in a MOF.  $^2\text{H}$  NMR line shape analysis revealed that the type of motion of the 2-mIM linker in ZIF-8 is preserved after amorphization. In contrast, the  $T_1$  and  $T_2$  measurements of  $a_m$ ZIF-8 revealed that the amorphization could significantly change the rotational angle, the activation barriers, and the rate constants for the original modes of motions in ZIF-8. Moreover, from the results of  $T_1$  and  $T_2$  measurement, we discovered the presence of the new librational mode (iv) in  $a_m$ ZIF-8, which could not be observed in the crystalline phase. We believe that our findings provide valuable insight into the changes induced in the framework mobility in  $a_m$ MOF and could be useful in the development of new functional materials with intrinsic dynamic properties. Investigations into the dynamics of glassy MOFs<sup>35-37</sup> is our next challenge.

This work was supported by the Russian Science Foundation (Project No. 17-73-10135), JST ACCEL (No. JPMJAC1501), JST PRESTO (No. JPMJPR1514), and JSPS Research Fellowship (No. 17J10099) from JSPS. XAS experiments were performed at the BL14B2 of SPring-8 with the approval of JASRI (Proposal No. 2018B1728).

### Conflicts of interest

There are no conflicts to declare.

### Notes and references

1. T. Akutagawa, H. Koshinaka, D. Sato, S. Takeda, S. Noro, H. Takahashi, R. Kumai, Y. Tokura and T. Nakamura, *Nat. Mater.*, 2009, **8**, 342.
2. T. Akutagawa, K. Shitagami, S. Nishihara, S. Takeda, T. Hasegawa, T. Nakamura, Y. Hosokoshi, K. Inoue, S. Ikeuchi, Y. Miyazaki and K. Saito, *J. Am. Chem. Soc.*, 2005, **127**, 4397.
3. M. Jin, T. S. Chung, T. Seki, H. Ito and M. A. Garcia-Garibay, *J. Am. Chem. Soc.*, 2017, **139**, 18115.

4. C. S. Vogelsberg and M. A. Garcia-Garibay, *Chem. Soc. Rev.*, 2012, **41**, 1892.
5. S. Horike, R. Matsuda, D. Tanaka, S. Matsubara, M. Mizuno, K. Endo and S. Kitagawa, *Angew. Chem. Int. Ed.*, 2006, **45**, 7226
6. D. I. Kolokolov, H. Jobic, A. G. Stepanov, V. Guillerme, T. Devic, C. Serre and G. Férey, *Angew. Chem. Int. Ed.*, 2010, **49**, 4791.
7. M. Inukai, T. Fukushima, Y. Hijikata, N. Ogiwara, S. Horike and S. Kitagawa, *J. Am. Chem. Soc.*, 2015, **137**, 12183.
8. J. D. Xiao, Q. Shang, Y. Xiong, Q. Zhang, Y. Luo, S. H. Yu and H. L. Jiang, *Angew. Chem. Int. Ed.*, 2016, **55**, 9389.
9. S. Bracco, F. Castiglioni, A. Comotti, S. Galli, M. Negroni, A. Maspero and P. Sozzani, *Chem. Eur. J.*, 2017, **23**, 11210.
10. M. Inukai, M. Tamura, S. Horike, M. Higuchi, S. Kitagawa and K. Nakamura, *Angew. Chem. Int. Ed.*, 2018, **57**, 8687.
11. N. B. Shustova, T. C. Ong, A. F. Cozzolino, V. K. Michaelis, R. G. Griffin and M. Dincă, *J. Am. Chem. Soc.*, 2012, **134**, 15061.
12. J. A. Rodriguez-Velamazán, M. A. Gonzalez, J. A. Real, M. Castro, M. C. Muñoz, A. B. Gaspar, R. Ohtani, M. Ohba, K. Yoneda, Y. Hijikata, N. Yanai, M. Mizuno, H. Ando and S. Kitagawa, *J. Am. Chem. Soc.*, 2012, **134**, 5083.
13. T. D. Bennett and A. K. Cheetham, *Acc. Chem. Res.*, 2014, **47**, 1555.
14. W. Chen, S. Horike, D. Umeyama, N. Ogiwara, T. Itakura, C. Tassel, Y. Goto, H. Kageyama and S. Kitagawa, *Angew. Chem. Int. Ed.*, 2016, **55**, 5195.
15. S. Tominaka, H. Hamoudi, T. Suga, T. D. Bennett, A. B. Cairns and A. K. Cheetham, *Chem. Sci.*, 2015, **6**, 1465.
16. T. D. Bennett, A. L. Goodwin, M. T. Dove, D. A. Keen, M. G. Tucker, E. R. Barney, A. K. Soper, E. G. Bithell, J. C. Tan and A. K. Cheetham, *Phys. Rev. Lett.*, 2010, **104**, 115503.
17. A. W. Thornton, K. E. Jelfs, K. Konstantas, C. M. Doherty, A. J. Hill, A. K. Cheetham and T. D. Bennett, *Chem. Commun.*, 2016, **52**, 3750.
18. T. D. Bennett, P. J. Saines, D. A. Keen, J. C. Tan and A. K. Cheetham, *Chem. Eur. J.*, 2013, **19**, 7049.
19. C. Orellana-Tavra, E. F. Baxter, T. Tian, T. D. Bennett, N. K. Slater, A. K. Cheetham and D. Fairen-Jimenez, *Chem. Commun.*, 2015, **51**, 13878.
20. T. D. Bennett, S. Cao, J. C. Tan, D. A. Keen, E. G. Bithell, P. J. Beldon, T. Friscic and A. K. Cheetham, *J. Am. Chem. Soc.*, 2011, **133**, 14546.
21. X. C. Huang, Y. Y. Lin, J. P. Zhang and X. M. Chen, *Angew. Chem. Int. Ed.*, 2006, **45**, 1557.
22. K. S. Park, Z. Ni, A. P. Côté, J. Y. Choi, R. Huang, F. J. Uribe-Romo, H. K. Chae, M. O'Keeffe and O. M. Yaghi, *Proc. Natl. Acad. Sci. USA*, 2006, **103**, 10186.
23. T. D. Bennett, J. Sotelo, J.-C. Tan and S. A. Moggach, *CrystEngComm*, 2015, **17**, 286.
24. W. Morris, C. J. Stevens, R. E. Taylor, C. Dybowski, O. M. Yaghi and M. A. Garcia-Garibay, *J. Phys. Chem. C*, 2012, **116**, 13307.
25. D. I. Kolokolov, A. G. Stepanov and H. Jobic, *J. Phys. Chem. C*, 2015, **119**, 27512.
26. A. Knebel, B. Geppert, K. Volgmann, D. I. Kolokolov, A. G. Stepanov, J. Twiefel, P. Heitjans, D. Volkmer and J. Caro, *Science*, 2017, **358**, 347.
27. Q. Song, S. K. Nataraj, M. V. Roussanova, J. C. Tan, D. J. Hughes, W. Li, P. Bourgoïn, M. A. Alam, A. K. Cheetham, S. A. Al-Muhtaseb and E. Sivaniah, *Energy Environ. Sci.*, 2012, **5**, 8359.
28. S. Chaemchuen, Z. Luo, K. Zhou, B. Mousavi, S. Phatanasri, M. Jaroniec and F. Verpoort, *J. Catal.*, 2017, **354**, 84.
29. G. Lu and J. T. Hupp, *J. Am. Chem. Soc.*, 2010, **132**, 7832.
30. S. Cao, T. D. Bennett, D. A. Keen, A. L. Goodwin and A. K. Cheetham, *Chem. Commun.*, 2012, **48**, 7805.
31. T. Friščić, I. Halasz, P. J. Beldon, A. M. Belenguer, F. Adams, S. A. J. Kimber, V. Honkimäki and R. E. Dinnebier, *Nat. Chem.*, 2012, **5**, 66.
32. H. W. Spiess, in *NMR: Basic Principles and Progress*, ed. P. Diehl, E. Fluck and R. Kosfeld, Springer-Verlag, New York, 1978, vol. 15, p 55–214.
33. D. I. Kolokolov, A. G. Maryasov, J. Ollivier, D. Freude, J. Haase, A. G. Stepanov and H. Jobic, *J. Phys. Chem. C*, 2017, **121**, 2844.
34. A. G. Redfield, *Adv. Magn. Opt. Reson.*, 1965, **1**, 1.
35. D. Umeyama, S. Horike, M. Inukai, T. Itakura and S. Kitagawa, *J. Am. Chem. Soc.*, 2015, **137**, 864.
36. A. Qiao, T. D. Bennett, H. Tao, A. Krajnc, G. Mali, C. M. Doherty, A. W. Thornton, J. C. Mauro, G. N. Greaves and Y. Yue, *Sci. Adv.*, 2018, **4**, eaao6827.
37. T. D. Bennett and S. Horike, *Nat. Rev. Mater.*, 2018, **3**, 431.

**A table of contents entry:**

We investigated the effect of amorphization on the mobility of the organic linkers in a metal-organic framework.

